JACS
JOURNAL OF THE AMERICAN CHEMICAL SOCIETY
Article
pubs.acs.org/JACS

Nanoscale Phase Separation in Sequence-Defined Peptoid Diblock Copolymers

Jing Sun,[†,‡] Alexander A. Teran,[§,∥] Xunxun Liao,[⊥,#] Nitash P Balsara,*[,‡,§,∥] and Ronald N. Zuckermann*[,†,‡]

[†]Molecular Foundry, [‡]Materials Sciences Division, [∥]Environmental Energy Technologies Division, and [#]National Center for Electron Microscopy, Lawrence Berkeley National Laboratory, Berkeley, California 94720, United States

[§]Department of Chemical and Biomolecular Engineering and [⊥]Department of Materials Science and Engineering, University of California, Berkeley, California 94720, United States

Supporting Information

ABSTRACT: Microphase-separated block copolymer materials have a wide array of potential applications ranging from nanoscale lithography to energy storage. Our understanding of the factors that govern the morphology of these systems is based on comparisons between theory and experiment. The theories generally assume that the chains are perfectly monodisperse; however, typical experimental copolymer preparations have polydispersity indices (PDIs) ranging from 1.01 to 1.10. In contrast, we present a systematic study of the relationship between chemical structure and morphology in the solid state using peptoid diblock copolymers with PDIs of ≤1.00013. A series of comb-like peptoid block copolymers, poly(*N*-2-(2-(2-methoxyethoxy)ethoxy)ethylglycine)-*block*-poly(*N*-(2-ethylhexyl)glycine) (pNte-*b*-pNeh), were obtained by solid-phase synthesis. The number of monomers per chain was held fixed at 36, while the volume fraction of the Nte block (ϕ_{Nte}) was varied from 0.11 to 0.65. The experimentally determined order−disorder transition temperature exhibited a maximum at ϕ_{Nte} = 0.24, not ϕ_{Nte} = 0.5 as expected from theory. All of the ordered phases had a lamellar morphology, even in the case of ϕ_{Nte} = 0.11. Our results are in qualitative disagreement with all known theories of microphase separation in block copolymers. This raises new questions about the intertwined roles of monomer architecture and polydispersity in the phase behavior of diblock copolymers.

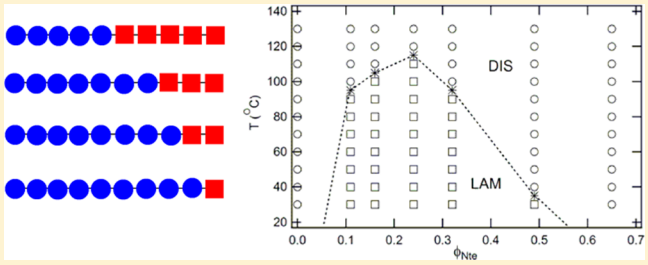

INTRODUCTION

Microphase-separated block copolymer materials have a wide array of potential applications ranging from nanoscale lithography to energy storage.[1,2] The relationship between the molecular structure and solid-state morphology of A−B diblock copolymers has been the subject of numerous theoretical studies.[3−6] At high temperatures, a disordered phase is obtained because of the dominance of entropic contributions. At low temperatures, a variety of ordered phases such as lamellae, a bicontinuous gyroid phase, cylinders arranged on a hexagonal lattice, and spheres arranged on a body-centered-cubic lattice are predicted depending on the chain length and the volume fraction of each block. These theories are remarkably general and cover a broad class of chemical structures. No distinction is made between polymers with branched monomers such as polystyrene, poly(ethyl ethylene), and poly(*n*-butyl acrylate), and linear polymers with unbranched monomers such as poly(ethylene oxide) and poly(1,4-butadiene).[7−13] Furthermore, the theories also adequately explain the behavior of polydisperse polymer preparations obtained by anionic or controlled radical polymerization methods, which typically generate samples with polydispersity indices (PDIs) ranging from 1.01 to 1.10.

Biologically inspired polymers, particularly polypeptoids, provide a convenient platform for exerting precise control over the block copolymer structure. Polypeptoids are a family of comb-like polymers based on nitrogen-substituted glycine monomers.[14,15] The iterative solid-phase submonomer synthesis method allows for the efficient synthesis of polymers with exact monomer sequences from an extremely diverse set of possible side-chain functionalities.[16,17]

One might think that peptide-based polymers with PDIs of 1.0, made by genetic engineering techniques,[18] are also ideally suited for fundamental studies of block copolymer self-assembly. The self-assembly of these materials in the bulk, however, is dominated by chain stiffness and hydrogen-bonding interactions, resulting in the formation of secondary structures such as α-helices and β-sheets.[19] Peptide-based polymers also exhibit limited solubility in commonly used solvents. In contrast, the peptoid-based polymers used in the present study have flexible backbones, dissolve readily in commonly used solvents, and do not contain backbone hydrogen-bond donors.[20] These properties make them excellent candidates for

Received: April 28, 2013
Published: September 3, 2013

dx.doi.org/10.1021/ja404233d | J. Am. Chem. Soc. 2013, 135, 14119−14124

investigating block copolymer self-assembly. In an important study, Rosales et al. studied the self-assembly of a diblock copolymer comprising a polystyrene block synthesized by anionic polymerization and a poly(*N*-(2-methoxy)ethylglycine) block synthesized by solid-phase synthesis. They obtained hexagonally packed cylindrical and lamellar morphologies, in good agreement with the classical block copolymer phase diagram.[21]

Here we study the solid-state morphology in a series of polypeptoid diblock copolymers where the degree of polymerization (N) was fixed at 36 and the PDIs were less than 1.00013. All previous studies of block-copolymer phase behavior involved samples with different values of N and significantly larger PDIs. Here, we designed a series of purified sequence-defined diblock copolymers, poly(*N*-2-(2-(2-methoxyethoxy)ethoxy)ethylglycine)-*block*-poly(*N*-(2-ethyl)-hexylglycine) (pNte-*b*-pNeh). The pNte phase enables the use of these materials as electrolytes in lithium batteries.[22] We show that precise control over the atomic structure provides unique insight into the impact of side-chain functionality and block-copolymer composition on morphology. Moreover, the characteristic dimensions of microphase separation are in the range of 6.2−7.1 nm, showing a sub-10-nm phase separation that is rarely observed in typical diblock copolymers.[23,24] We believe that our study prompts reexamination of the relationship between monomer structure and self-assembled morphologies in nearly monodisperse block copolymers.

RESULTS AND DISCUSSION

In this work, we designed and synthesized a series of sequence-defined poly(*N*-(2-(2-(2-methoxyethoxy)ethoxy)ethyl)-glycine)-*block*-poly(*N*-(2-ethylhexyl)glycine) (pNte-*b*-pNeh) block copolymers. The molecular structure of the copolymers is shown schematically in Figure 1. The total chain length was fixed at 36 monomers for all molecules studied, and the volume fraction of the Nte block was varied from 0.11 to 0.65 (Table 1).

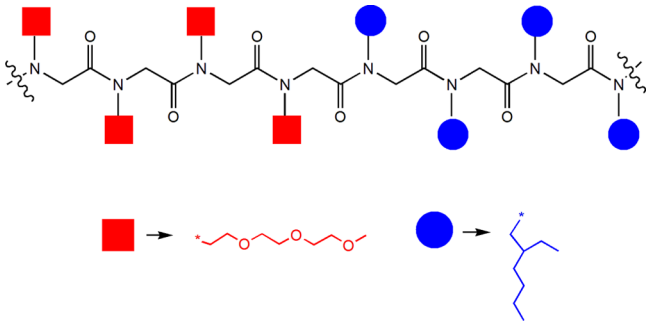

Figure 1. Schematic of pNte-*b*-pNeh block copolypeptoids. The blue circles represent *N*-(2-ethylhexyl)glycine (Neh), and the red squares represent *N*-2-(2-(2-methoxyethoxy)ethoxy)ethylglycine (Nte).

The thermal properties of the polymers were first investigated by differential scanning calorimetry (DSC) (Figure S2a, Supporting Information). The lack of melting peaks and crystallization exotherms indicates that $pNeh_{20}$ and all of the pNeh-*b*-pNte copolymers are noncrystalline. This is consistent with previous results.[22] Moreover, the absence of Bragg peaks in the XRD patterns of pNeh-*b*-pNte confirms the lack of a crystalline structure (Figure S2b, Supporting Information). These results suggest that both blocks in this diblock copolymer are amorphous. Note that the pNeh block side chain has a chiral center and is a mixture of two enantiomers (Figure S3, Supporting Information).

Table 1. Characteristics of the Block/Homo Polypeptoid $(Nte)_m-(Neh)_n$ Synthesized

m	n	ϕ_{Nte}	molar mass (calc/obs) (g/mol)	purity[a] (%)	PDI[b]
24	12	0.65	6966.6/6964.0	82	1.00012
18	18	0.49	6762.8/6762.7	96	1.00004
12	24	0.32	6559.0/6562.9	97	1.00003
9	27	0.24	6457.1/6456.8	>95[c]	1.00005
6	30	0.16	6355.1/6364.6	>95[c]	1.00005
4	32	0.11	6287.2/6297.3	>95[c]	1.00005
0	20	0	3444.0/3431.0	96	1.00001

[a]Purity was determined by analytical high-performance liquid chromatography (HPLC). [b]PDI was determined by matrix-assisted laser desorption/ionization (MALDI) analysis and purity (see Supporting Information). [c]As estimated by MALDI analysis.

The phase behavior of the pNeh-*b*-pNte polymers was studied by small-angle X-ray scattering (SAXS). In Figure 2, we

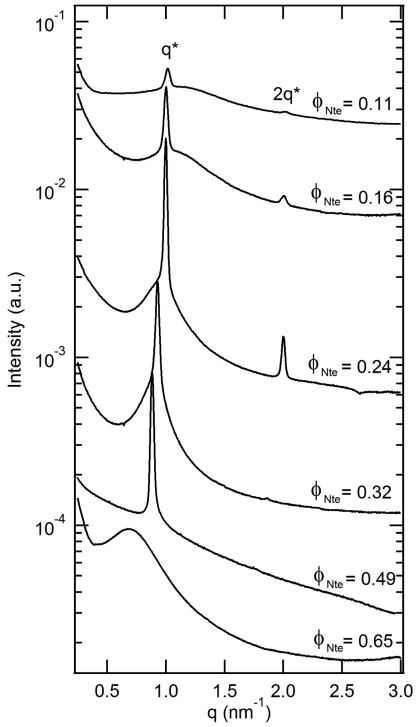

Figure 2. SAXS profiles at room temperature for pNte-*b*-pNeh with different chain lengths. Profiles are vertically offset for clarity.

show SAXS profiles obtained at 25 °C. The SAXS profile of the sample with ϕ_{Nte} = 0.65 contains one broad scattering peak, indicating that the sample is disordered. All of the other samples exhibit a sharp primary peak at $q = q^*$, indicating an ordered phase. Higher-order peaks at $q = 2q^*$, indicating a lamellar phase, were seen in all of the ordered samples except the sample with ϕ_{Nte} = 0.49. The missing higher-order peak in the sample with ϕ_{Nte} = 0.49 is expected because of the symmetric nature of the copolymer. The center-to-center distance between adjacent pNte lamellae, d, is given by $d = 2\pi/q^*$. The values of d thus obtained are given in Table 2. It is evident that d decreases from 7.1 to 6.2 as ϕ_{Nte} decreases from

dx.doi.org/10.1021/ja404233d | J. Am. Chem. Soc. 2013, 135, 14119−14124

Table 2. Characteristics of the Block Copolymers pNte-*b*-pNeh Obtained by SAXS and Theoretical Predictions[a]

ϕ_{Nte}	T_{ODT} (°C)	d (nm)	N^* at T_{ODT}	C	χ at T_{ODT}	b (nm)
0.65	–	–	101	–	–	–
0.49	35	7.1	107	10.9	0.103	0.49
0.32	95	6.7	107	13.5	0.125	0.50
0.24	115	6.3	109	18.9	0.173	0.49
0.16	105	6.3	110	33.9	0.310	0.53
0.11	95	6.2	110	66.0	0.600	0.55

[a] d is the center-to-center distance between adjacent pNte lamellae. N^* is the total number of repeat units per chain, relative to the 0.1 nm^3 reference volume. C is described in eq 1. χ is the Flory–Huggins parameter. b is the statistical segment length.

0.49 to 0.11. This is consistent with the classical theory of Leibler.[3] Interestingly, all of the domain spacings are below 10 nm in the experimental window, which has rarely been observed in classic block copolymers.[25,26] This is due to the low molar mass of our samples and their low polydispersity.[27,28]

We show SAXS profiles obtained from the sample with ϕ_{Nte} = 0.16 as a function of temperature in Figure 3. Sharp primary

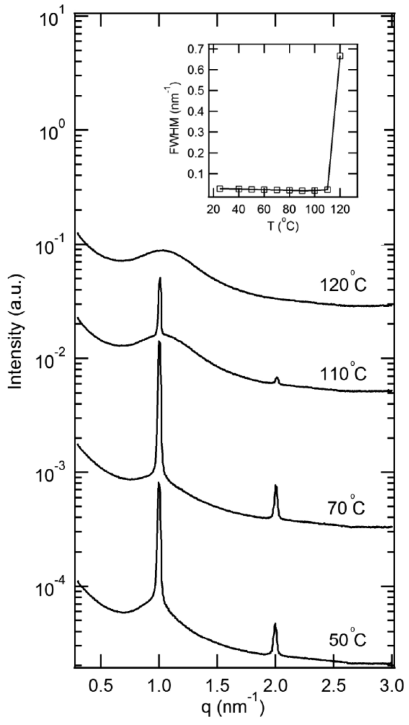

Figure 3. SAXS intensity versus scattering vector, q, for $pNte_6$-*b*-$pNeh_{30}$ at selected temperatures. The inset is a plot of the full width at half-maximum (fwhm) of the primary peak of the SAXS profiles as a function of temperature. Profiles are vertically offset for clarity.

scattering peaks are seen at and below 110 °C. An abrupt transition from order to disorder was seen when the sample was heated from 110 to 120 °C. The full width at half-maximum (fwhm) of the primary peak is plotted as a function of temperature in the inset of Figure 3. The abrupt increase in fwhm between 110 and 120 °C is taken as a signature of the order-to-disorder transition, and the transition temperature, T_{ODT}, is assumed to be 115 °C. Similar SAXS experiments were conducted on all of the samples listed in Table 1, and the results are summarized in Figure 4. The phase behavior of

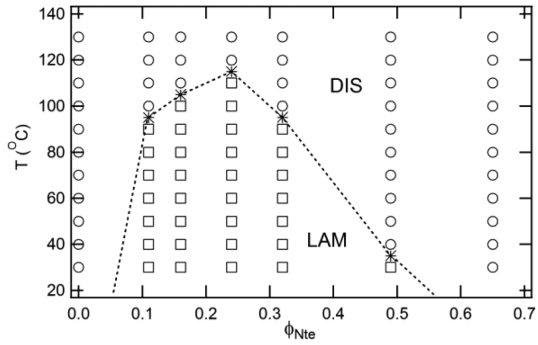

Figure 4. Phase diagram of pNte-*b*-pNeh at various temperatures and volume fractions of pNte (ϕ_{Nte}), where DIS is the disordered phase and LAM is the lamellar phase. The stars represent the order–disorder temperature, and the dotted line represents estimated locations of phase boundaries.

pNte-*b*-pNeh copolymers with $m + n = 36$ is surprisingly simple. Only disordered and lamellar phases are obtained; peaks at $2^{1/2}$, $3^{1/2}$, $5^{1/2}$, and $6^{1/2}$ that are standard signatures of nonlamellar structures in conventional block copolymers are entirely absent in the present system, regardless of composition and temperature. The lamellar phase obtained in the sample with ϕ_{Nte} = 0.24 is stable up to 115 °C, whereas in the sample with ϕ_{Nte} = 0.49, it is stable up to 35 °C. The classical theory of Leibler[3] predicts that the ordered phases formed in the sample with ϕ_{Nte} = 0.49 should be more stable than those formed in the sample with ϕ_{Nte} = 0.24. It is clear that our experimental results are not in an agreement with Leibler's theory.[3] In fact, the dependence of T_{ODT} on ϕ_{Nte} shown in Figure 4 is not consistent with any of the theories on block copolymer self-assembly. Similarly, the absence of hexagonally packed cylinders (i.e., the absence of a Bragg peak at $q = 3^{1/2}q^*$) and other morphologies in Figure 4 is entirely surprising.

The distinguishing feature of our work is the fact that $m + n$ was held fixed, that is, the total number of chemical repeat units per chain, $N = m + n$, is constant. All other studies of the phase behavior of block copolymers as a function of composition are based on samples with substantially different N values; see, for example, refs 11 and 29. It is customary to combine results obtained from such samples by converting measured T_{ODT} values into χ values assuming a function of the form $\chi = A + B/T$ where A and B are constants, independent of block copolymer composition and molecular weight. It is important to note that the phase diagram in Figure 4 is not based on this assumption.

The reason for the unusual phase behavior of pNte-*b*-pNeh copolymers is not clear at this stage. Our copolymers have relatively long comb-like branches emanating from each monomer. This could, in principle, increase the stiffness of the chains, which, in turn, can stabilize the lamellar phase in highly asymmetric block copolymers.[30,31] Recent SANS[20,32] and NMR spectroscopy[33] data suggest that the peptoid backbone is inherently flexible because of the lack of main-chain chirality and a hydrogen-bond donor. It was shown that the persistence lengths of (*R*)-*N*-(1-phenylethyl)glycine-containing polypeptoids ranged from 0.5 to 1 nm, which is quite low and similar to that of polystyrene (1 nm).[34] A crude measure of chain stiffness was obtained by analyzing SAXS patterns obtained from disordered pNte-*b*-pNeh copolymers using Leibler's theory.[3] The location of the disordered scattering peak was used to determine the statistical segmental

dx.doi.org/10.1021/ja404233d | J. Am. Chem. Soc. 2013, 135, 14119–14124

length of the copolymers, b. (We used Figure 2 in ref 3 and assumed that the two blocks had the same statistical segmental length.) We used a reference volume of 0.1 nm^3 as the basis for our calculations. The total numbers of repeat units per chain based on this reference volume, N^*, for all of our samples are given in Table 2. Values of b, obtained by comparing our SAXS data with Leibler's predictions,[3] are also included in Table 2. It is evident from Table 2 that b ranges from 0.49 to 0.55 nm. These values are very similar to those of conventional polymers (b for polystyrene is reported to be 0.5 nm[35]). It is thus unlikely that chain stiffness is the reason for the unexpected phase behavior of pNte-*b*-pNeh reported in Figure 4.

If the lamellae were composed of pure pNeh and pNte chains, then only Bragg peaks would be expected in the SAXS profiles. In contrast, several SAXS patterns from the copolymers studied here have Bragg peaks superposed on a more diffuse background; see the ϕ_{Nte} = 0.16 data in Figure 2 and the 110 °C data in Figure 3. We attribute this fact to the presence of pNeh chains in the pNte-rich domains (and the concomitant presence of pNte chains in the pNeh-rich domains) in the vicinity of the ODT. Note the similarity of the diffuse background at 110 °C and the SAXS pattern from the fully disordered $pNte_6$-*b*-$pNeh_{30}$ sample in Figure 3. To our knowledge, the superposition of Bragg peaks on a diffuse background has not been reported in any previous study on pure block copolymer melts. It is likely that the unusual properties of peptoid block copolymers arise because of their extremely low polydispersity.

In Leibler's theory,[3] the product χN^* at the spinodal, which we assume is the ODT, is a constant C that depends on ϕ_{Nte} (see Figure 4 in ref 3)

$$\chi N^* = C(\phi_{Nte}) \quad (1)$$

where χ is the Flory–Huggins parameter (e.g., C = 10.5 when ϕ_{Nte} = 0.5). (We ignore effects due to differences in the statistical segment lengths of pNte and pNeh.) We estimated χ at T_{ODT} using eq 1, and the results are shown in Table 2. As can be seen from Table 2, samples with ϕ_{Nte} ranging from 0.32 to 0.11 have T_{ODT} values in a relatively narrow range (95–115 °C) despite the fact that the expected χN^* value at the ODT increases from 13.5 to 66.0. It is thus conceivable that the unexpected phase behavior seen in Figure 4 is due to a composition-dependent χ parameter. Another possibility is that the thermodynamic behavior of block copolymers is fundamentally affected by the chemical structure of the monomers. The blocks of our peptoid-based copolymers have chemically identical hydrophilic backbones; the only difference is the chemical identity of the branches (hydrophilic versus hydrophobic) as shown schematically in Figure 1. It is conceivable that the thermodynamic properties of such materials are very different from those of conventional block copolymers in which both the backbone and the branches of the blocks are chemically distinct.

Several studies have addressed the phase behavior of block copolymers that are closely related to our peptoid-based comb-like systems.[5,21,36−46] Much of this work has focused on block copolymers with one comb-like block and one coil block.[38−43] Although the phase diagram of these systems differ substantially from those of coil–coil diblock copolymers, cylindrical microphases with curved interfaces were reported in all cases. This is true of the experimental works reported by Ruokolainen et al.,[36] Runge et al.,[37] and Pulamgatta et al.,[41] as well as the theoretical works reported by Kriksin et al.[40] and Wang et al.[41] Soo et. al studied the properties of poly(lauryl methacrylate)-*block*-poly[oligo(oxyethylene)methacrylate] copolymers (PLMA-*b*-POEM).[45] Only one sample was reported to exhibit a lamellar morphology. Rzayev[46] studied a bottlebrush diblock copolymer with polymethacrylate as the backbone and polystyrene and polylactide as the side chains for each block and observed exclusively the formation of lamellae with a polylactide volume fraction in the range of 0.29–0.43. (We use the term bottlebrush to describe monomers with long, polymerized side chains.) He hypothesized that the semirigid nature of the polymer chain was responsible for this phase behavior. Whereas the formation of curved interfaces in peptide-containing block copolymers has been reported,[44] block copolymers with a polypeptide block and a coil block exhibit lamellar morphologies over a wide range of compositions (polypeptide volume fractions between 0.15 and 0.75).[45] This is driven by the crystallization of the polypeptide blocks into α-helices and β-sheets. Similarly, lamellar phases dominate the phase behavior of copolymers with a semicrystalline block such as polyethylene.[47−50] It should be evident from this discussion that the phase behavior in Figure 4 is distinct from that observed in all previous studies of block copolymer phase behavior. A common feature of the experimental work is that it was conducted on samples with significantly higher PDIs than our samples. Whether this is responsible for the observed phase behavior is not clear.

Extension of the theoretical work of Kriksin et al. might provide a more rational explanation for the phase behavior in Figure 4.[40] They used self-consistent field theory to study microphase separation in diblock copolymers with amphiphilic monomers. They defined an amphiphilic monomer as one in which the backbone is very different from the pendant group (e.g., a hydrophilic backbone and a hydrophobic pendant group). All other theories on block copolymer self-assembly ignore the structure and composition of the monomers.[3,4,6−13] In contrast, Kriksin et al. explicitly accounted for the chemical structure of comb-like monomers. The molecules that they examined were similar to that in the cartoon used to describe our pNte-*b*-pNeh copolymers (Figure 1). The difference is that the theory considers copolymers in which only one of the blocks is amphiphilic and comb-like. One would thus obtain the copolymer described by Kriksin et al. by eliminating the red squares in our cartoon in Figure 1. Note that the peptoid backbone with a pendant CH_3 group is water-soluble;[51] in contrast, the pendant 2-ethylhexyl group (blue circles in Figure 1) is hydrophobic. The morphologies of copolymers with one amphiphilic block, predicted in ref 40, are similar to those of conventional block copolymers. Predicted morphologies include lamellae, the cubic gyroid phase, cylinders arranged on a hexagonal lattice, and spheres arranged on a body-centered-cubic lattice. It is conceivable that the extension of this model to include hydrophilic pendant groups on the hydrophilic coil block would lead to predictions consistent with our experiments. The amphiphilic nature of the monomers might induce local structures that are very different from those seen in conventional random coils.

■ CONCLUSIONS

A series of comb-like diblock copolypeptoids, poly(*N*-2-(2-(2-methoxyethoxy)ethoxy)ethylglycine)-*block*-poly(*N*-(2-ethylhexyl)glycine) (pNte-*b*-pNeh), with precisely defined sequences were synthesized by solid-phase synthesis. The chain length of all samples in this study was fixed at 36

dx.doi.org/10.1021/ja404233d | J. Am. Chem. Soc. 2013, 135, 14119−14124

monomers per chain, and the volume fraction of the Nte block, ϕ_{Nte}, was varied from 0.11 to 0.65. Only lamellar and disordered morphologies were observed over the entire composition and temperature window examined. The domain spacing was found to decrease from 7.1 to 6.2 nm as ϕ_{Nte} was decreased from 0.49 to 0.11, in agreement with classical theory. However, a plot of the experimentally determined order−disorder transition temperature versus ϕ_{Nte} exhibited a peak at $\phi_{Nte} = 0.24$, instead of $\phi_{Nte} = 0.5$ as expected from the theory. This might be due to a composition-dependent χ parameter or the amphiphilic nature of the peptoid monomers. The ability to fine-tune the intra- and intermolecular interactions makes the peptoid system an excellent platform for fundamental studies of block copolymer self-assembly. We hope that such systematic studies will, in the long run, enhance our understanding of the relationship between monomer structure and self-assembled morphologies in nearly monodisperse block copolymers.

■ ASSOCIATED CONTENT

Supporting Information

MALDI mass spectra, differential scanning calorimetry, X-ray diffraction, and circular dichroism data for polypeptoids. This material is available free of charge via the Internet at http://pubs.acs.org.

■ AUTHOR INFORMATION

Corresponding Author

*nbalsara@berkeley.edu; rnzuckermann@lbl.gov

Notes

The authors declare no competing financial interest.

■ ACKNOWLEDGMENTS

Funding for this work was provided by the Soft Matter Electron Microscopy Program, supported by the Office of Science, Office of Basic Energy Science, U.S. Department of Energy, under Contract xDE-AC02-05CH11231. The work was carried out at the Molecular Foundry at Lawrence Berkeley National Laboratory, supported by the Office of Science, Office of Basic Energy Science, U.S. Department of Energy, under Contract DE-AC02-05CH11231. We thank Dr. Daniel Hallinan and Dr. Adrianne M. Rosales for helpful advice and Dr. Babak Sanii for help with XRD on the project.

■ REFERENCES

(1) Singh, M.; Odusanya, O.; Wilmes, G. M.; Eitouni, H. B.; Gomez, E. D.; Patel, A. J.; Chen, V. L.; Park, M. J.; Fragouli, P.; Iatrou, H.; Hadjichristidis, N.; Cookson, D.; Balsara, N. P. *Macromolecules* **2007**, *40*, 4578−4585.

(2) Ruiz, R.; Kang, H.; Detcheverry, F. A.; Dobisz, E.; Kercher, D. S.; Albrecht, T. R.; de Pablo, J. J.; Nealey, P. F. *Science* **2008**, *321*, 936−939.

(3) Leibler, L. *Macromolecules* **1980**, *13*, 1602−1617.

(4) Fredrickson, G. H.; Helfand, E. *J. Chem. Phys.* **1988**, *89*, 5890.

(5) Khokhlov, A. R.; Khalatur, P. G. *Chem. Phys. Lett.* **2008**, *461*, 58−63.

(6) Matsen, M. W.; Bates, F. S. *Macromolecules* **1996**, *29*, 1091−1098.

(7) Floudas, G.; Ulrich, R.; Wiesner, U. *J. Chem. Phys.* **1999**, *110*, 652.

(8) Loo, Y.-L.; Register, R. A.; Ryan, A. J. *Macromolecules* **2002**, *35*, 2365−2374.

(9) Bates, F. S. *Science* **1991**, *251*, 898.

(10) Bates, F. S.; Fredrickson, G. H. *Phys. Today* **1999**, *52*, 32−38.

(11) Floudas, G.; Vazaiou, B.; Schipper, F.; Ulrich, R.; Wiesner, U.; Iatrou, H.; Hadjichristidis, N. *Macromolecules* **2001**, *34*, 2947−2957.

(12) Epps Iii, T. H.; Bailey, T. S.; Waletzko, R.; Bates, F. S. *Macromolecules* **2003**, *36*, 2873−2881.

(13) Groot, R. D.; Madden, T. J. *J. Chem. Phys.* **1998**, *108*, 8713.

(14) Zuckermann, R. N. *Pept. Sci.* **2011**, *96*, 545−555.

(15) Rosales, A. M.; Segalman, R. A.; Zuckermann, R. N. *Soft Matter* **2013**, *9*, 8400−8414.

(16) Sun, J.; Zuckermann, R. N. *ACS Nano* **2013**, *7*, 4715−4732.

(17) Zuckermann, R. N.; Kerr, J. M.; Kent, S. B. H.; Moos, W. H. *J. Am. Chem. Soc.* **1992**, *114*, 10646−10647.

(18) van Hest, J. C. M.; Tirrell, D. A. *Chem. Commun.* **2001**, 1897−1904.

(19) Lecommandoux, S.; Achard, M.-F.; Langenwalter, J. F.; Klok, H.-A. *Macromolecules* **2001**, *34*, 9100−9111.

(20) Rosales, A. M.; Murnen, H. K.; Kline, S. R.; Zuckermann, R. N.; Segalman, R. A. *Soft Matter* **2012**, *8*, 3673−3680.

(21) Rosales, A. M.; McCulloch, B. L.; Zuckermann, R. N.; Segalman, R. A. *Macromolecules* **2012**, *45*, 6027−6035.

(22) Sun, J.; Stone, G. M.; Balsara, N. P.; Zuckermann, R. N. *Macromolecules* **2012**, *45*, 5151−5156.

(23) Radzilowski, L. H.; Stupp, S. I. *Macromolecules* **1994**, *27*, 7747−7753.

(24) Beiner, M.; Huth, H. *Nat. Mater.* **2003**, *2*, 595−599.

(25) Stupp, S. I.; LeBonheur, V.; Walker, K.; Li, L.-S.; Huggins, K. E.; Keser, M.; Amstutz, A. *Science* **1997**, *276*, 384−389.

(26) Wanakule, N. S.; Panday, A.; Mullin, S. A.; Gann, E.; Hexemer, A.; Balsara, N. P. *Macromolecules* **2009**, *42*, 5642−5651.

(27) Li, S.; Register, R. A.; Landes, B. G.; Hustad, P. D.; Weinhold, J. D. *Macromolecules* **2010**, *43*, 4761−4770.

(28) Lynd, N. A.; Hillmyer, M. A. *Macromolecules* **2005**, *38*, 8803−8810.

(29) Khandpur, A. K.; Foerster, S.; Bates, F. S.; Hamley, I. W.; Ryan, A. J.; Bras, W.; Almdal, K.; Mortensen, K. *Macromolecules* **1995**, *28*, 8796−8806.

(30) Olsen, B. D.; Segalman, R. A. *Mater. Sci. Eng. R: Rep.* **2008**, *62*, 37−66.

(31) Olsen, B. D.; Shah, M.; Ganesan, V.; Segalman, R. A. *Macromolecules* **2008**, *41*, 6809−6817.

(32) Murnen, H. K.; Rosales, A. M.; Dobrynin, A. V.; Zuckermann, R. N.; Segalman, R. A. *Soft Matter* **2013**, *9*, 90−98.

(33) Sui, Q.; Borchardt, D.; Rabenstein, D. L. *J. Am. Chem. Soc.* **2007**, *129*, 12042−12048.

(34) Brulet, A.; Boue, F.; Cotton, J. P. *J. Phys. II* **1996**, *6*, 885−891.

(35) Eitouni, H. B.; Balsara, N. P. In *Physical Properties of Polymers Handbook*; Springer: New York, 2007; pp 339−356.

(36) Ruokolainen, J.; Saariaho, M.; Ikkala, O.; Ten Brinke, G.; Thomas, E. L.; Torkkeli, M.; Serimaa, R. *Macromolecules* **1999**, *32*, 1152−1158.

(37) Runge, M. B.; Lipscomb, C. E.; Ditzler, L. R.; Mahanthappa, M. K.; Tivanski, A. V.; Bowden, N. B. *Macromolecules* **2008**, *41*, 7687−7694.

(38) Nandan, B.; Lee, C.-H.; Chen, H.-L.; Chen, W.-C. *Macromolecules* **2005**, *38*, 10117−10126.

(39) Pulamagatta, B.; Pankaj, S.; Beiner, M.; Binder, W. H. *Macromolecules* **2011**, *44*, 958−965.

(40) Kriksin, Y. A.; Khalatur, P. G.; Erukhimovich, I. Y.; Ten Brinke, G.; Khokhlov, A. R. *Soft Matter* **2009**, *5*, 2896−2904.

(41) Wang, L.; Lin, J.; Zhang, L. *Langmuir* **2009**, *25*, 4735−4742.

(42) Minich, E. A.; Nowak, A. P.; Deming, T. J.; Pochan, D. J. *Polymer* **2004**, *45*, 1951−1957.

(43) Schlaad, H.; Smarsly, B.; Losik, M. *Macromolecules* **2004**, *37*, 2210−2214.

(44) Papadopoulos, P.; Floudas, G.; Schnell, I.; Aliferis, T.; Iatrou, H.; Hadjichristidis, N. *Biomacromolecules* **2005**, *6*, 2352−2361.

(45) Soo, P. P.; Huang, B.; Jang, Y. I.; Chiang, Y. M.; Sadoway, D. R.; Mayes, A. M. *J. Electrochem. Soc.* **1999**, *146*, 32−37.

(46) Rzayev, J. *Macromolecules* **2009**, *42*, 2135−2141.

(47) Mai, S. M.; Fairclough, J. P. A.; Viras, K.; Gorry, P. A.; Hamley, I. W.; Ryan, A. J.; Booth, C. *Macromolecules* **1997**, *30*, 8392−8400.

(48) Parras, P.; Castelletto, V.; Hamley, I. W.; Klok, H. A. *Soft Matter* **2005**, *1*, 284−291.
(49) Rangarajan, P.; Register, R. A.; Fetters, L. J.; Bras, W.; Naylor, S.; Ryan, A. J. *Macromolecules* **1995**, *28*, 4932−4938.
(50) Quiram, D. J.; Richard, A.; Marchand, G. R. *Macromolecules* **1997**, *30*, 4551−4558.
(51) Lau, K. H. A.; Ren, C.; Sileika, T. S.; Park, S. H.; Szleifer, I.; Messersmith, P. B. *Langmuir* **2012**, *28*, 16099−16107.